Measurement of Ion Number Density and Velocity Distribution in an Anode-layer Type Hall Thruster by Laser Induced Florescence Method

IEPC-2009-149

Presented at the 31st International Electric Propulsion Conference,
University of Michigan • Ann Arbor, Michigan • USA
September 20 – 24, 2009

Shigeru Yokota[1], Kentaro Hara[2], Shinatora Cho[3], Daisuke Takahashi[4], Kimiya Komurasaki[5], Yoshihiro Arakawa[6]
The University of Tokyo, Bunkyo, Tokyo,113-0033, Japan

Abstract: The discharge oscillation of an anode-layer type Hall thruster is one of the most serious problems to be overcome. In general, a hollow anode is used in order to stabilize the operation. Recent numerical simulation results show the stable operation depends on the ionization rate in the hollow anode. In order to verify the simulation result, it is needed to measure the plasma profile in the hollow anode. In this paper, as a first step, the number density and the velocity distribution of single-charged xenon ions in an anode-layer type Hall thruster were investigated by means of Laser-Induced Fluorescence (LIF) for the $5d^2F_{7/2}\rightarrow 6p^2D^0_{5/2}$ excitation transition at 834.7 nm detecting the non-resonant line to the $6s^2P_{3/2}$ state at 541.9 nm. As a result, we obtained the relative ion number density and the velocity distributions. The ion velocity distribution function shows both ionization and acceleration occur in the acceleration channel, while only ionization occurs in the hollow anode.

Nomenclature

B	=	magnetic flux density
c	=	speed of light
D	=	hollow anode width
F	=	total angular momentum quantum number
g	=	Lande-factor
h	=	Planck constant
I	=	nuclear angular moment quantum number
J	=	total electronic moment quantum number
M	=	magnetic quantum number
P	=	relative intensity
v	=	velocity
μ_B	=	Bohr magnetron
ν	=	frequency
z	=	axial position
Z	=	acceleration channel length

[1] Assistant Professor, Department of Aeronautics and Astronautics, yokota@al.t.u-tokyo.ac.jp
[2] Graduate Student, Department of Aeronautics and Astronautics, hara@al.t.u-tokyo.ac.jp
[3] Graduate Student, Department of Aeronautics and Astronautics, cho@al.t.u-tokyo.ac.jp
[4] Graduate Student, Department of Aeronautics and Astronautics, takahashi@al.t.u-tokyo.ac.jp
[5] Professor, Department of Advanced Energy, komurasaki@k.u-tokyo.ac.jp
[6] Professor, Department of Aeronautics and Astronautics, arakawa@al.t.u-tokyo.ac.jp

Subscripts
0 = static state
i = index

I. Introduction

A Hall thruster is one of the most promising electric propulsion system for the satellite station keeping or orbit transfer maneuvering because it produces high thrust efficiency with a specific impulse range of 1,000 ~ 3000 s.[1,2] An anode-layer type Hall thruster has higher thrust density and efficiency than the other type, magnetic layer type Hall thruster. However an anode-layer type Hall thruster also has a serious problem of discharge current oscillation.[3] Therefore, it has never loaded on satellites yet in practical use.

In general, a hollow anode[4] is used in order to stabilize the discharge oscillation. However, even when the hollow anode is used, stable operation range is still narrow. Recent numerical studies[5] show the stable operation depends on the ionization rate in the hollow anode. The purpose of this study is to measure the plasma profile in the hollow anode in order to verify the numerical simulation results. In this paper, the excited ion number density distribution and ion energy function distribution were measured by Laser-Induced fluorescence (LIF) method.

II. Theory

A. Lase-induced fluorescence

LIF can be subdivided in two subsequent processes, namely photon absorption and spontaneous emission. Therefore a laser is tuned in frequency over a certain transition frequency and the fluorescence signal is monitored. It has to be taken into account that due to the Doppler effect the absorption frequency of particles moving in the direction of the laser beam is shifted proportional to the relative velocity between the particle and the laser. This shift in frequency is calculated according to

$$\Delta\nu = \nu_0 \frac{v}{c}. \tag{1}$$

B. Hyperfine structure

Xenon naturally occurs in nine isotopes. The different mass and nuclear charge distribution depending on the number of neutrons leads to slightly different transition energies for the isotopes and thus to a profile splitting in nine lines. Table 1 gives a summary of the natural abundance of the Xe+ ions and the shift of the line relative to Xe132. Unfortunately experimental data for the isotope shift of the $5d\ ^2F_{7/2} \rightarrow 6p\ 2D^0_{5/2}$ transition is not available. Following the approach of Manzella[6] and others experimental data of the similar $5d\ 4D_{7/2} \rightarrow 6p\ 4P^0_{5/2}$ was used[7,8].

Further splitting into a hyperfine structure occurs for the isotopes with non-zero nuclear spin, Xe129 and Xe131, due to nucleon-electron spin interaction producing a total of 19 lines. The quantum number that accounts for this effect is the total angular momentum quantum number F that takes values according to

$$F = I + J, I + J - 1, ..., |I - J|. \tag{2}$$

The selection rules state that only transitions with $\Delta F = \pm 1,0$ are possible with the exception that $\Delta F = 0$ is not allowed for F=0. The relative intensity of the isotope shifted transitions can be calculated according to their natural abundance. As for the hyperfine structure, quantum mechanical considerations yield calculation formulas[9] for the relative intensities of the transitions that have to be multiplied with the abundance of the isotope.

In presence of a magnetic field of sufficient strength the Zeeman effect should be considered. It leads to further splitting of the hyperfine structure symmetric to the original lines. The magnetic quantum number M signifies the projection of F on the magnetic axis and takes values from

$$M = -F, -F + 1, ..., F - 1, F. \tag{3}$$

The general selection rule is $\Delta M = \pm 1,0$. Applying this rule for the 9 isotopes of xenon produces a total of 432 lines. The frequency for all this transitions can be calculated according to

$$\nu = \nu_0 + \mu_B B \frac{g'M' - g''M''}{h}. \tag{4}$$

was taken from the tables provided by Candler[6].

Broadening mechanisms are not separately accounted for since they are overlaid by the line broadening due to the variation in velocity caused by spatial extent of the ionization region.

The resulting line shape is a superposition of 432 transition lines broadened due to the velocity distribution by the Doppler effect. By assuming a suitable velocity distribution function it is possible to reconstruct this complex line shape. For the presented work the function

$$f(\nu) = \sum_i H(-\tilde{\nu}) \cdot I_i \cdot \tilde{\nu}_i^2 \cdot \exp\left[-\frac{\tilde{\nu}_i^2}{E_0}\right]. \tag{5}$$

was used, with the abbreviation, as

$$\tilde{\nu} = \nu - \Delta\nu_i - \nu_0. \tag{6}$$

Here $\Delta\nu$ denotes the line shift and ν_0 and E_0 are fitting parameters. The index i represents the m summation over all 432 hyperfine and Zeeman split components. $H(-\tilde{\nu})$ denotes the Heaviside step function that returns 1 for positive and 0 for negative arguments. It is used to suppress the second arm of the chosen fitting function. The reasons for choosing this function are quite straightforward. It is a well-known fact that skewed velocity distribution functions in which the most probable and the statistical mean velocity differ significantly are characteristic for Hall effect thrusters. Furthermore the discharge voltage constitutes a clear upper limit for the ion energy.

Table 1 Isotope splitting.

Isotope	Abundance %	Shift in MHz
Xe^{124}	0.096	336.6
Xe^{126}	0.09	252.4
Xe^{128}	1.92	172.0
Xe^{129}	26.4	113.7
Xe^{130}	4.1	83.6
Xe^{131}	21.1	16.7
Xe^{132}	26.9	0
Xe^{134}	10.4	-75.8
Xe^{136}	8.9	-140.9

III. Experiment

A. Anode-layer-type Hal thruster

Figure 1 shows the cross-section of a 1 kW class anode layer type Hall thruster.[10] The inner and outer diameters of the acceleration channel are 48 mm and 72 mm, respectively. A solenoid coil is set at the center of the thruster to apply a radial magnetic field in the acceleration channel. The magnetic flux density is varied by changing the coil current. The guard rings are made of stainless steel, which is applied the cathode voltage. It has a hollow anode through which a propellant gas is fed. The width of the hollow anode is 8 mm and the gap between the anode tip and the exit plane of the acceleration channel is 3 mm. Xenon is used as a propellant. A hollow cathode is used as the electron source. A normal operating condition is tabulated in Table 2.

The experiments were conducted in the vacuum chamber of the University of Tokyo with a diameter of 2 meters and a length of 3 meters. The vacuum is achieved by the employment of two rotary pumps (250 l/s), a mechanical booster pump (2800 l/s) and a diffusion pump (3700 l/s).

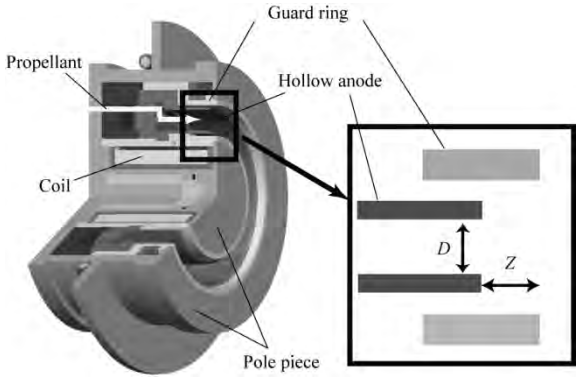

Figure 1. Anode-layer type Hall thruster.

Table 2. Typical operation parameter.

Parameter	Value
Propellant Gas	Xenon
Mass flow rate	1.36 mg/s
Discharge voltage	250 V
Discharge current	1.1 A
Applied magnetic field	14 mT
Back pressure	2.9 x 10^{-3} Pa

B. Optical system

The optical system was set up according to Fig. 2. The exciting laser beam is directed on the acceleration channel through the viewport of the vacuum chamber and modulated by a mechanical chopper. This modulation is necessary to provide a reference for the separation of the LIF signal and the natural emission of the Xenon plasma by means of a lock-in amplifier. The diode laser is set to the desired wavelength by temperature control and then fine tuned by the use of a function generator controlling the laser working current. Optical feedback that might lead to mode hopping in the diode laser is prevented by a Faraday isolator. For the monitoring of the current wavelength emitted by the diode laser a spectrometer was utilized. The fluorescence signal is detected by a collection optic that is movable in the thruster's axial direction. Through an optical fiber the signal reaches the lock-in amplifier after being filtered by a band pass filter and being converted to an electrical signal by a photomultiplier. An etalon with a free spectral range of 0.75 GHz was deployed as a fine wave meter. For the recording of the signal a digital oscilloscope with a resolution of 10 bit was used.

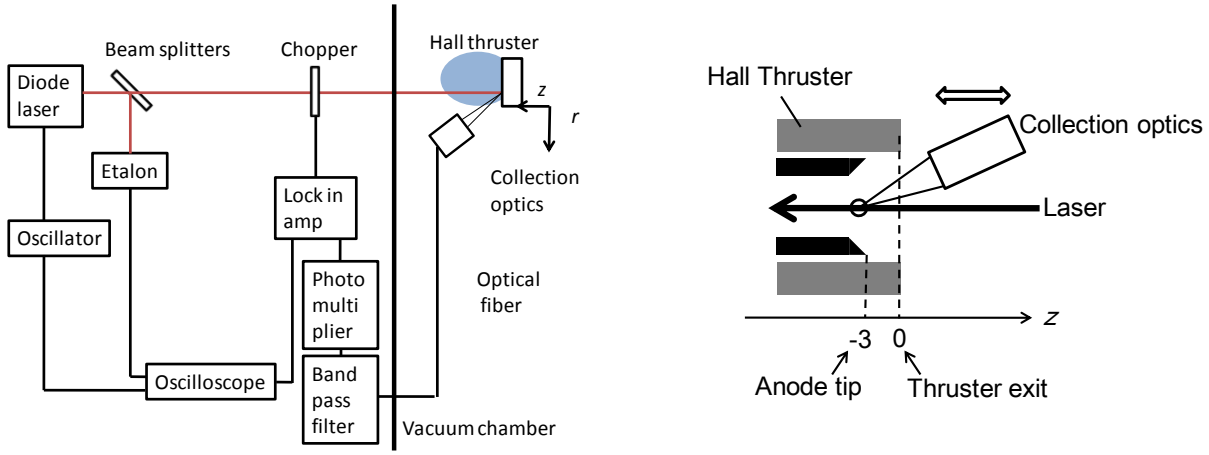

Figure 2. Optical setup.

IV. Result and Discussion

A. LIF profile

Figure 3 shows one of the obtained line spectra and the result for the fitting function given in equation (5). The good agreement between fitting function and LIF signal attests the general suitability of the function class with its free parameters. Furthermore the detailed consideration of numerous splitting effects provides a solid physical basis for the fitting. Here the Zeeman effect is neglected because the maximum line shifts due to hyperfine splitting are -3.05 GHz and 1.84 GHz. On the other hand the maximum values for the Zeeman splitting are below ±0.4 GHz.

The relative number density can be obtained from the integration of the profile. The velocity distribution function is obtained by deconvoluting the profile using the fitting function.

B. Ion energy distribution

Figure 4 shows the ion velocity distributions. In the stable operation case (a), the velocity distribution broadening in the plume (z<+2 mm) was much larger than that in the Hall thruster. This result indicates that only low energy ions exist from inside of the anode hollow to the discharge channel (z < 0) because only ionization occurs in this region, while high energy ion also exist in the outside of the Hall thruster because both ionization and acceleration occur in this region. In other words, the ionization region spread in the Hall thruster while the acceleration area locates on the outside. On the other hand, in the oscillative operation case (b), the velocity distributions have a certain degree of broadenings in the discharge channel (z >-2 mm). In this case, ions are accelerated in the discharge channel.

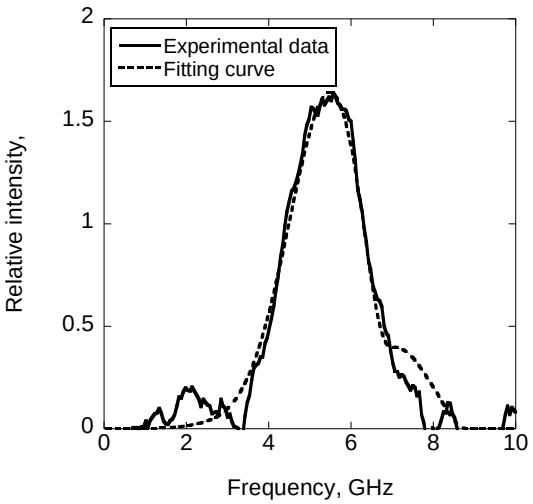

Figure 3. LIF signal and its fitting function for a typical operation condition.

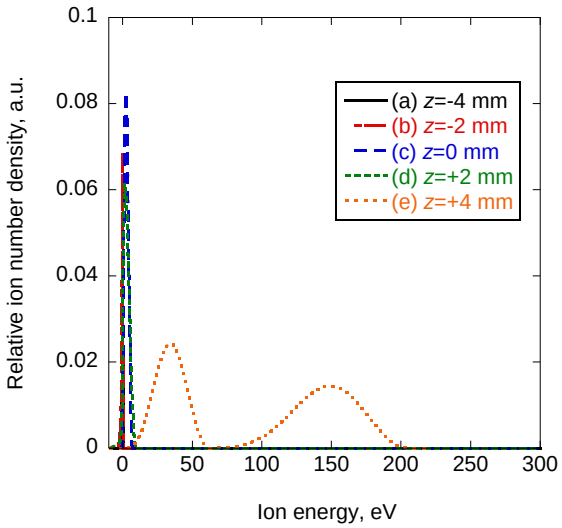

(a) B_0 = 10 mT

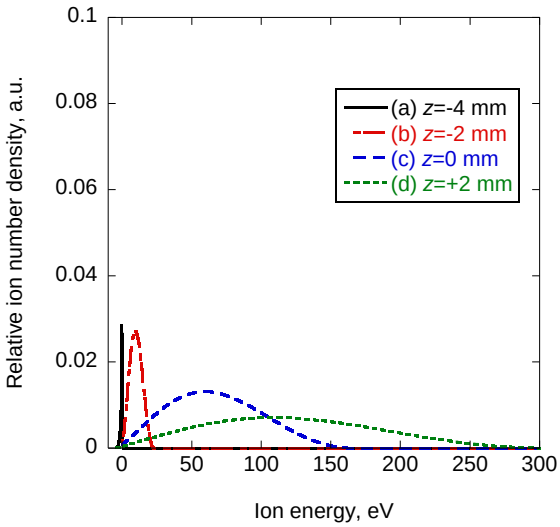

(b) B_0 = 20 mT

Figure 4. Ion energy distribution *V_d=250 V, $\dot{m}$=1.36 mg/s.*

C. Electric potential and ion number density distribution

From the ion energy distribution, the potential distribution was calculated (Fig. 5 (a)). As shown in this figure, the potential drop located on the outside of the thruster in the stable operation case (B_0=10 mT), while located in the discharge channel in the oscillative operation case (B_0=20 mT). This result is similar to the numerical simulation result (b).[5]

In the calculation result, the maximum potential value was more than 300 V at B_0=10 mT, while it was several volts higher than the anode voltage in the experimental result. In addition, the location of the potential drop was in the thruster in the calculation result, while it was in the outside of the thruster in the experimental result. These seem to be caused by the narrowness of the calculation region. In the calculation, the electrical potential is fixed at 0 V.

Figure 6 shows the relative ion number density distributions. Because of the lack of the reference cell to calibrate the absolute ion number density, the measured distribution (a) has no unit. The operation was stable at B_0=10 mT while the discharge oscillation was observer at B_0 = 25 mT. The ion number density at B_0=25 mT is time averaged

value because the discharge oscillation frequency (1-10 kHz) is much higher than the sampling rate of the equipments.

As shown in Fig. 6 (a), the ion number density in the case of stable operation (B=10 mT) was larger than that in the case of the oscillative operation (B=20 mT) in the whole region. The tendency corresponded with that shown in the calculated result (b).[5]

The difference of the ion number density between two cases in the measured result is smaller than that in the calculation result. This is obviously caused by the higher potential value in the calculation result. To improve the calculation result, the calculation region should be expanded.

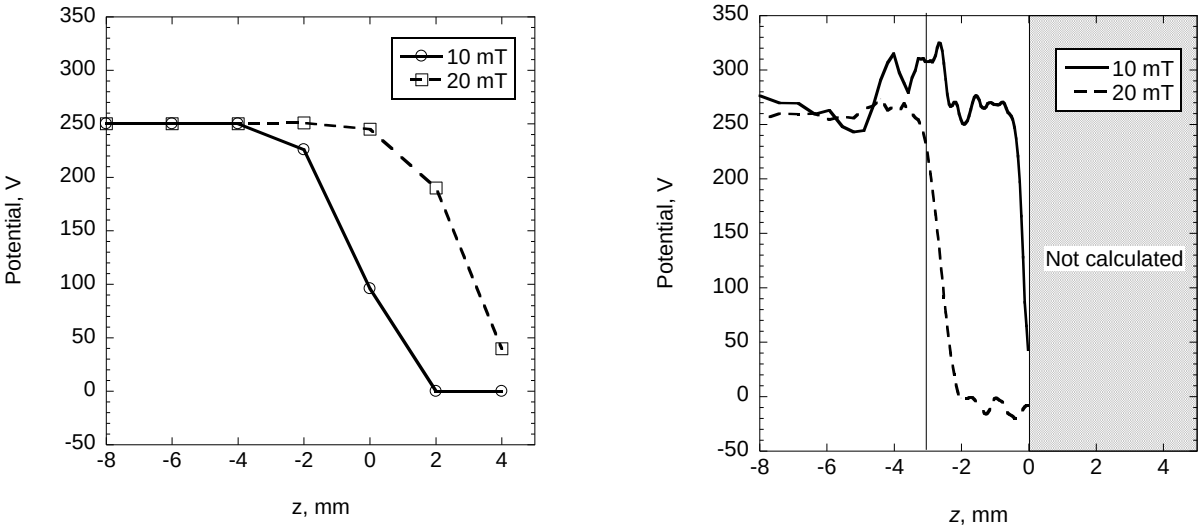

(a) Measured (b) Calculated

Figure 5. Potential distribution V_d=250 V, $\dot{m}$=1.36 mg/s.

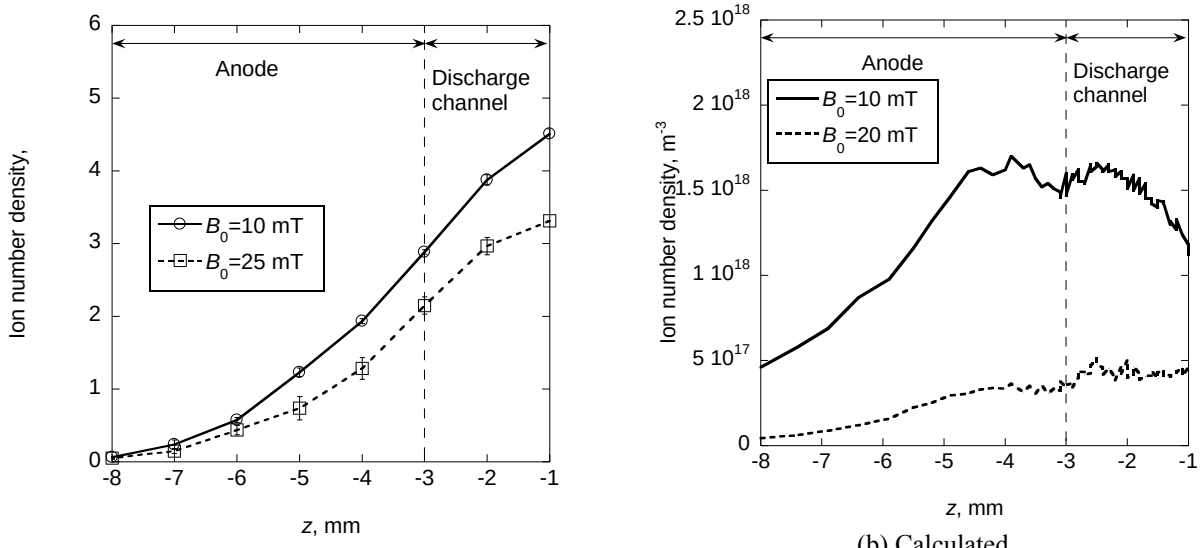

(a) Measured (b) Calculated

Figure 6. Ion number density distribution V_d=250 V, $\dot{m}$=1.36 mg/s.

V. Conclusion

The ion number density and ion velocity in the anode-layer type Hall thruster were measured using LIF spectroscopy. The results are as follows:

1) The ion number density in the case of stable operation (B_0=10 mT) is larger than that in the case of the oscillative operation (B_0=20 mT) in the whole region.

2) The ion velocity distribution functions indicated that the ionization region spreads from the anode hollow to the discharge channel and the acceleration region locates on the outside in the stable operation case, while both ionization and acceleration occurs in the discharge channel in the oscillative operation case.

3) The potential drop locates in the outside in the stable operation case. On the other hand, the potential drop locates on the discharge channel.

The calculation result was validated by these measurement results.

References

[1] Boyd, I. D., "Review of Hall Thruster Plume Modeling", *Journal of Spacecraft and Rockets*, Vol. 38, No. 5, 2001, pp. 381-387.

[2]Oh, D. Y., Hastings, D. E., Marrese, C. M., Haas, J. M., and Gallimore, A. D., "Modeling of Stationary Plasma Thruster Plumes and Implications for Satellite Design," *Journal of Propulsion and Power*, Vol. 15, No. 2, 1999, pp. 345-357.

[3]E. Choueiri, "Plasma oscillation in Hall Thrusters," *Physics of Plasmas*, Vol.8, 4, 2001, pp. 1411-1426

[4]A. V. Semenkin, S. O. Tverdokhlebov, V. I. Garkusha, A. V. Kochergin, G. O. Chislov, B. V. Shumkin, A. V. Solodukhin, L. E. Zakharenkov, "Operating Envelopes of Thruster with Anode Layer," IEPC-Paper 2001-13, 2001.

[5]S. Yokota, K. Komurasaki, Y. Arakawa "Numerical Analysis of Anode Sheath Structure Transition in an Anode-layer Type Hall Thruster," IEPC Paper 2007-095, 2007.

[6]Manzella, D. H., "Stationary Plasma Thruster Ion Velocity Distribution", Proceedings of the 30th Joint Propulsion Conference, AIAA-94-3141, 1994

[7]Bingham, C. R., Gaillard, M. L., Pegg, D.J., Carter, H. K., Mlekodaj, R. L., Cole, J. D., Griffin, P. M, "Collinear Fast-Beam Laser Spectroscopy Experiment: Measurement of Hyperfine Structure and Isotope Shifts in Xe II", *Nuclear Instruments and Methods* 202, 1982, pp. 147-152.

[8]Borghs, G., De Bisschop, P., Silerans, R. E., van Hove, M., van den Cruyce, J. M., „Hyperfine structures and isotope shifts of the 5d 4D7/2 □ 6p 4P05/2 transition in xenon ions", *Zeitschrift für Physik* A 299, 1981, pp. 11-13.

[9]Candler, C., "Atomic Spectra", 2nd edition, Hilger & Watts, 299-330 (1964)

[10]Yamamoto, N. Komurasaki, K., Arakawa, Y., "Discharge Current Oscillation in Hall Thrusters", *Journal of Propulsion and Power*, Vol. 21, No. 5, 2005, pp. 870-876.